Behaviour & Information Technology, Vol. 24, No. 3, May–June 2005, 161 – 173

Taylor & Francis
Taylor & Francis Group

Image pre-compensation to facilitate computer access for users with refractive errors

M. ALONSO Jr.†*, A. BARRETO‡, J. G. CREMADES§, J. A. JACKO¶ and M. ADJOUADI§

†Digital Signal Processing Laboratory, Florida International University, Miami, FL 33174 USA
‡Electrical and Computer Engineering Department/Biomedical Engineering Department, Florida International University, Miami, FL 33174 USA
§School of Human Performance and Leisure Sciences, Barry University, Miami Shores, FL 33161 USA
¶School of Industrial Systems Engineering, Georgia Institute of Technology, Atlanta, GA 30332, USA

Computer technologies, frequently employed for everyday tasks, often use Graphical User Interfaces (GUIs), presented through monitors or LCD displays. This type of visual interface is not well suited for users with refractive visual limitations, particularly when they are severe and not correctable by common means. In order to facilitate computer access for users with refractive deficiencies, an algorithm has been developed, using *a priori* knowledge of the visual aberration, to generate on-screen images that counter the effect of the aberration. When the user observes the screen displaying a pre-compensated image, the image perceived in the retina will be similar to the original image. The algorithm was tested by artificially introducing a spherical aberration in the field of view of 14 subjects, totaling 28 individual eyes. This use of pre-compensation improves the visual performance of the subjects with respect to that achieved with no compensation.

Keywords: Point spread function; Retina; Deconvolution; Pre-deblurring; Human-computer interface; Refractive error; Wavefront abberation; Image processing; Universal access

1. Introduction

In interacting with computers, human beings rely heavily on their sense of vision. Thus, if there are any aberrations present in a user's visual system, his/her effective use of the personal computer is hindered. This, in turn, restricts those users in many of their everyday activities. Optical lenses have been used to overcome visual limitations, such as defocus, in one way or another since the 13th century. Developments in ophthalmology during the last century have arisen to compensate for these aberrations in the form of contact lenses, and recently, Laser-Assisted *In Situ* Keratomileusis (LASIK) surgery. These forms of correction, however, can only deal with what are known as low-order aberrations. They are ill-suited to deal with high-order aberrations, characteristic, for example, of a corneal degeneration know as keratoconus (Parker and Parker 2002).

There have been attempts to compensate for the high-order visual aberrations in the human eye (Liang *et al.* 1997, Thibos *et al.* 1999, Higuchi *et al.* 2000). These methods however, are bulky and require very expensive, customized equipment. Thibos *et al.* (1999) propose the use of a spatial light modulator to provide the compensation, much the same way as glasses do. Liang *et al.* (1997) provide the compensation via a deformable mirror and an online method of measuring the aberration of the user. Although these methods are effective, their complexity and high cost render them impractical for everyday use.

In contrast with the optical correction of visual limitations, the approach described here is based on modifying the image at its source, i.e., applying image processing modifications on the image to be displayed on-screen before it is shown to the user, based on the knowledge of his/her own wavefront aberration function. Additionally, this method should apply equally well to

*Corresponding author. Email: miguel.alonso@fiu.edu

Behaviour & Information Technology
ISSN 0144-929X print/ISSN 1362-3001 online © 2005 Taylor & Francis Group Ltd
http://www.tandf.co.uk/journals
DOI: 10.1080/01449290412331327456

both low-order (myopia, hyperopia, etc.) as well as high order aberrations (e.g., keratoconus). The aim of the pre-compensation proposed is to modify the intended display image in a way that is opposite to the effect of the wavefront aberration of the eye. Once this is achieved, the result is displayed to the viewer so that the wavefront aberration in the viewer's eye will 'cancel' the pre-compensation, resulting in the projection of an undistorted version of the intended image on the retina. The method outlined here could leverage the power of personal computers (PCs) already available to the intended users. Additionally, contemporary computer systems often include powerful high-end graphics cards whose resources could be used to implement practical pre-compensation techniques.

With knowledge of the user's visual aberration, it is possible to generate images to be displayed on-screen that pre-compensate for the aberration present in the user's eye, without requiring additional equipment.

The paper is organized as follows. We begin in section 2 by introducing the problem with examples presenting the degradation in image quality when aberrations are present. The approach proposed to compensate for these aberrations is then outlined in section 3, followed by a description of the procedure used in the evaluation of the proposed approach (section 4), and the results (section 5). Finally, in section 6 the conclusions are drawn.

2. Problem statement

Our visual perspective of the world is formed by the projection of the image of the objects in that world against the retina, the light sensitive portion of the human eye. The retina is composed of rods and cones, which generate action potentials when stimulated by light (Guyton and Hall 1996). The human eye, being an imaging system, behaves in a manner similar to any type of imaging system composed of lenses (Thibos 2000), which form an image at their effective focal length.

Any object, when being viewed by the eye, can be thought of as a two-dimensional array of points, each varying with intensity (Wilson 1995). Thus, for an aberration-free eye, each point in the object is represented as a point on the retina, at the focal length of the eye's lens. In the case of a human–computer interface, when the user views the computer screen, each pixel can be thought of as a point-source of light, and the corresponding image of that pixel is projected onto the retina.

If the eye is unable to project a point source of light onto the retina as a corresponding point, the result is a broad Point Spread Function (PSF), causing the point source of light to be projected not at one point, but rather at multiple points on the retina, which introduces a blurring effect in the retinal image (figure 1).

The PSF of a human eye can be found indirectly through its wavefront aberration function, which represents the deviation of the light wavefront from a purely spherical pattern as it passes the pupil on its way to the retina (Salmon 1999). In an unaberrated eye, the refracted light is organized in the form of a uniform spherical wavefront, converging to the paraxial focal point on the retina.

Modern day solutions are limited in that they can only offer corrections for those individuals whose visual impairments are not severe. But for some individuals whose visual impairments are very severe, a more robust system of visual compensation is necessary.

2.1 *The human eye as a linear shift-invariant system*

For many applications, optical systems can be thought of as Linear Shift-Invariant (LSI) systems (Goodman 1968), and the eye can also be modelled as one of these systems (Salmon 1999). In this context, this means that, irrespective of its position in the viewed scene, a point of light will cause the same type of blur (characterized by the PSF) in the corresponding location of the retina, and that the retinal image can be modelled as the summation of all the displaced PSFs that are caused and scaled by all the individual points of light making up the viewed scene. Within this framework, all of the rules that apply to conventional LSI systems also apply to the optical system.

Let us consider that the retinal image, $U'(x,y)$ is formed by the convolution of the system input, $U(x,y)$, with the system's two-dimensional impulse response, or PSF, $H(x,y)$:

$$U'(x,y) = U(x,y) \otimes H(x,y) \tag{1}$$

where $\otimes$ denotes convolution.

This model for the imaging process in optical systems can be applied to the eye and is widely accepted. It has been illustrated in numerous texts via simulation, in which an image is blurred by convolution with a broad PSF, representing a level of defocus (Salmon 1999, Thibos 2000) (figure 2). Under these same assumptions, the

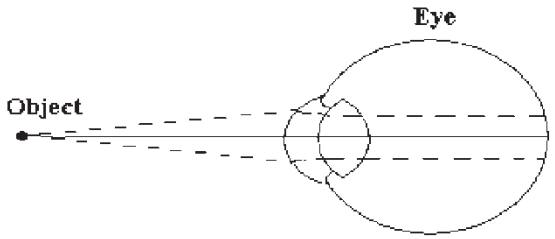

Figure 1. Spreading of a point object due to visual impairment.

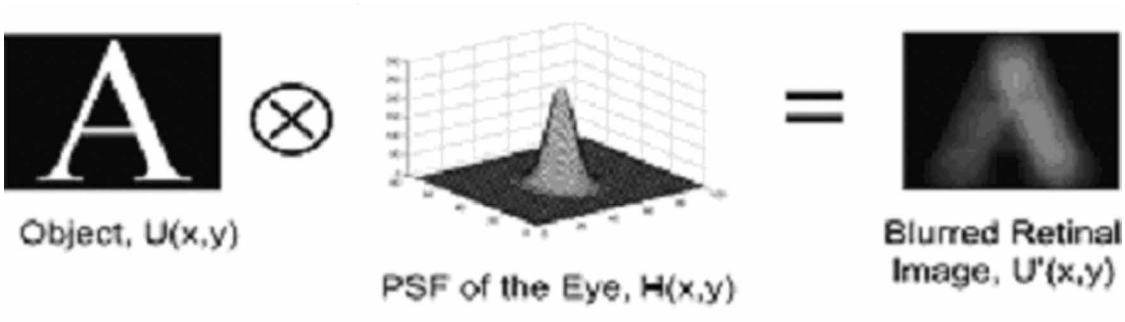

Figure 2. Block diagram of human eye as an LSI.

degraded retinal image can be reconstructed through an inverse process, given by

$$U(x,y) = U'(x,y) \otimes H^{-1}(x,y) \tag{2}$$

where $H^{-1}(x,y)$ is the inverse of the PSF.

This inverse process is referred to as 'deconvolution'. The process of deconvolution is the convolution of the blurred image with the inverse of the PSF. The deconvolution recovers the undistorted image. If instead, the deconvolution is applied to the undistorted image, a pre-compensated image will be created. When viewed through the PSF, this pre-compensated image will be projected onto the retina, free of distortion. This process is illustrated by

$$U(x,y) = (U(x,y) \otimes H^{-1}(x,y)) \otimes H(x,y). \tag{3}$$

To use computers efficiently, in addition to reading text, a user must be able to navigate in the GUI through the use of icons (Kline and Glinert 1995, Jacko *et al*. 2000). Figure 3 illustrates an example of what a user with a severe low-order aberration would face when interfacing with a computer via icons. The PSF used for this simulation is shown in figure 4. Figure 3b exemplifies the difficulty a user would face when trying to identify various icons to perform ordinary tasks.

Deconvolution does not have a precise mathematical definition and is reputed as mathematically ill-posed because it may yield multiple solutions. However, the practical importance of the deconvolution concept has prompted the design of several methods for its implementation (Gonsalves and Nisenson 1991).

3. Approach

Recently developed 'wavefront analysers' based on the Hartmann-Shack principle have made it possible to measure the wavefront aberration function for the human eye. These wavefront analysers are becoming common in many ophthalmologists' offices.

The wavefront aberration function, $W(x,y)$, is the primary component of the pupil function, $P(x,y)$, which incorporates the complete information about the imaging properties of the optical system (Williams and Becklund 1989). The pupil function is given by the following:

$$P(x,y) = A(x,y)e^{-j\cdot 2\cdot \pi \cdot n \cdot W(x,y)/\lambda} \tag{4}$$

where $A(x,y)$ is the amplitude function describing the relative efficiency of light passing through the pupil (usually given a value of one), n is the index of refraction, and λ is the wavelength of light in a vacuum (Salmon 1999).

According to the Fourier optics relationships in the eye, knowledge of the pupil function can be used to determine the optical transfer function (OTF) which is 'one of the most powerful descriptors of imaging performance for an optical system' (Williams and Becklund 1989). The OTF is a complex function whose magnitude is the modulation transfer function (MTF) and whose phase is the phase transfer function (PTF) (Salmon 1999).

The OTF can be found by convolving the pupil function, $P(x,y)$, with its complex conjugate, $P^*(-x,-y)$ (Goodman 1968, Wilson 1995, Salmon 1999, Thibos 2000):

$$O(fs,fy) = P(x,y) \otimes P^*(-x,-y). \tag{5}$$

This is equivalent of saying that the OTF is the autocorrelation of the pupil function. The PSF and the OTF are a Fourier transform pair (Wilson 1995):

$$O(fx,fy) = F\{H(x,y)\}. \tag{6}$$

Once the PSF is obtained for the user's eye, it is used in the deconvolution process.

The proposed pre-compensation of images requires the measurement of the PSF, the wavefront aberration function or the OTF of the viewer's eye. The solution to this complex instrumentation problem has evolved

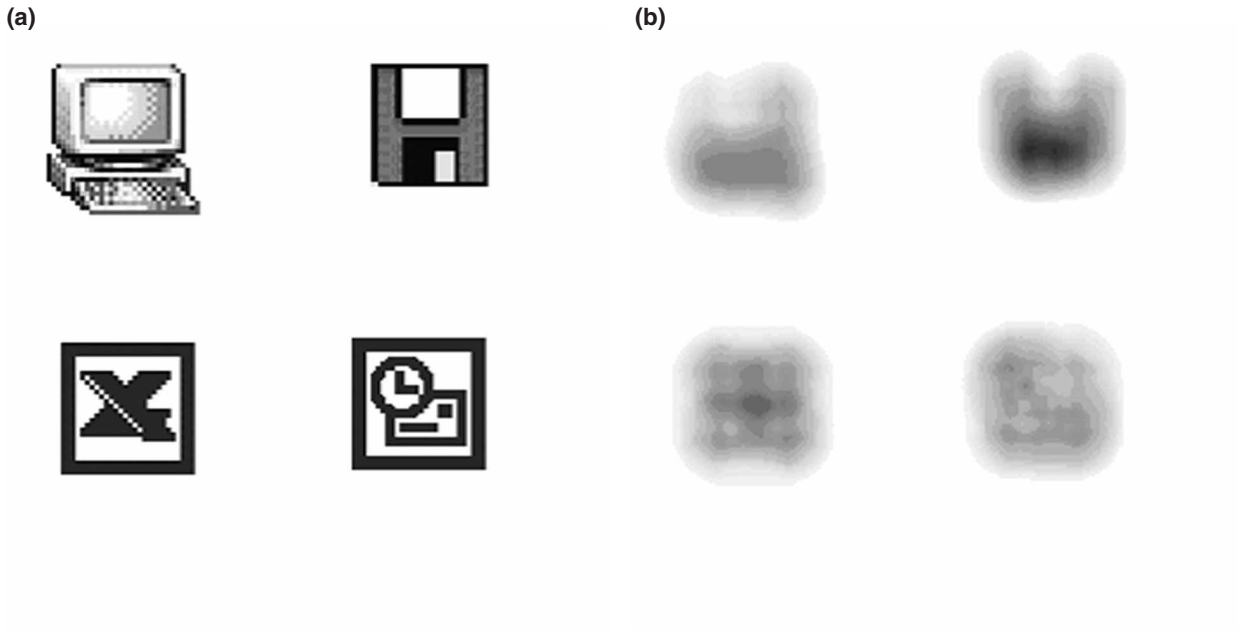

Figure 3(a). Icons displayed on a computer screen; (b) what the user with a severe spherical aberration would perceive.

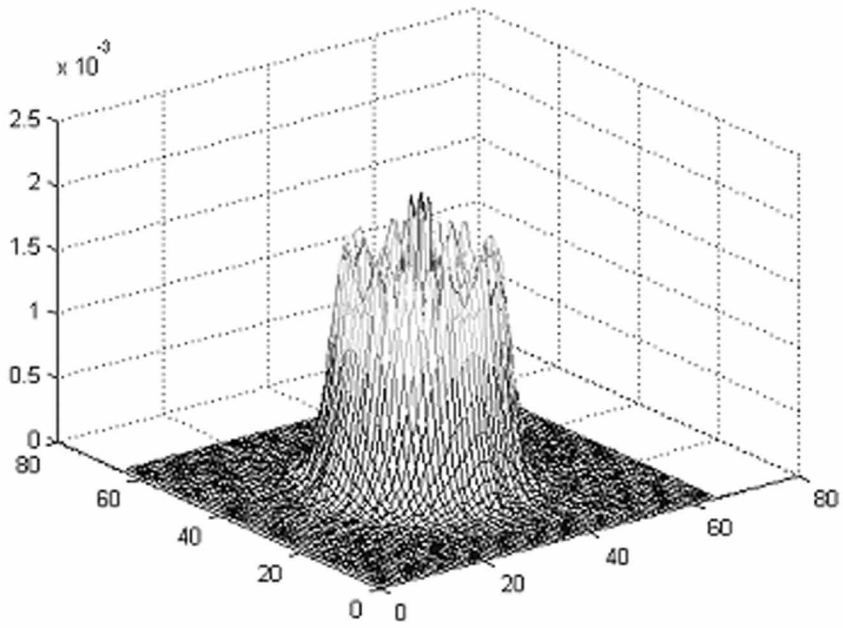

Figure 4. Broad PSF due to visual impairment.

steadily since the 1950s. In 1989, Williams and Becklund predicted that the usefulness of the OTF 'is here to stay, and it is being used to advantage in a number of practical ways. Therefore, we expect the art, at least in its application, will mature; and we anticipate not slowly'. Their expectations were fulfilled in 1994 when Liang *et al.* (1994) introduced an experimental system to measure the wavefront aberration of the human eye using the Hartmann-Shack principle. This same principle is currently applied in available turn-key wavefront analysers that have given rise to the so-called 'wavefront technology' in ophthalmology. This wavefront technology is 'an exciting, new field currently being developed in the ophthalmic community' (Hjortdal 2003). As such, wave-

front analysis technology is becoming a common element in the set of tools that many ophthalmologists or optometrists use for assessing the refractive errors of the eye (Young 2003). Thus, it is not unreasonable to expect that in the near future, patients will have access to their wavefront aberration information. This will allow for a customized pre-compensation scheme in their computers.

3.1 *Deconvolution overview*

Inverse filtering is traditionally used in image processing to restore an image $U(x,y)$ from a degraded image $G(x,y)$, assuming a known degradation function, $H(x,y)$ (Gonzales and Wood 2002). As stated above, the input and output of any linear system are related through the convolution operator. That is,

$$G(x,y) = U(x,y) \otimes H(x,y). \tag{7}$$

If the Fourier principles of convolution are applied, $U(x,y)$ can be obtained as follows:

$$U(x,y) = F^{-1}\left\{\frac{F\{G(x,y)\}}{F\{H(x,y)\}}\right\} \tag{8}$$

where $F\{\ \}$ and $F^{-1}\{\ \}$ denote the Fourier transform and the inverse Fourier transform, respectively.

In the context of pre-compensation of a digital image to be shown to the viewer, the objective is to deconvolve the PSF of the viewer's eye, $H(x,y)$, from the intended digital image, $I(x,y)$, in order to derive the pre-compensated display image to show on-screen, $RD(x,y)$. This calculation of $RD(x,y)$ is practically accomplished as:

$$RD(x,y) = F^{-1}\left\{\frac{F\{I(x,y)\}}{F\{H(x,y)\}}\right\}. \tag{9}$$

The denominator within the braces of equation (9) is the OTF of the viewer's eye.

This implementation of inverse filtering has several limitations, however, especially for values of the OTF which are close to zero. A common approach to circumvent this problem is the use of minimum mean square error (Weiner) filtering (Gonzales and Wood 2002). In the context of the problem at hand, this approach obtains the pre-compensated image as:

$$RD(fx,fy) = \left[\frac{1}{H(fx,fy)}\frac{|H(fx,fy)|^2}{|H(fx,fy)|^2 + K}\right] I(fx,fy) \tag{10}$$

where $RD(fx,fy)$, $H(fx,fy)$, and $I(fx,fy)$ are the Fourier transforms of $RD(x,y)$, $H(x,y)$, and $I(x,y)$, respectively, and K is a specified constant that affects the accuracy of the deconvolution.

For the example in figure 3, the simulated user's PSF is shown in figure 4. Following the method outlined above and applying it to figure 3a, a pre-deconvolved image is generated (figure 5a). This image is then viewed through the visual aberration. The result (figure 5b) shows that the pre-compensation has reverted some of the acuity loss introduced by the aberration. However, this figure also shows a loss of contrast due to the intensity scaling that must be applied to the pre-compensated image in order to display it on the computer monitor.

3.2 *Adaptive histogram equalization*

In order to overcome the loss of contrast introduced by the necessary intensity scaling, a suitable method of post processing must be employed. Contrast manipulation techniques provide the kind of enhancement required in this application. They consist of altering the grey levels of a digital image in such a way as to produce a 'better' image. In the context of this scheme, the 'better' image would be an enhanced version of the pre-compensated image, that when viewed through the aberration would be perceived with higher contrast than that of the just pre-compensated image. The expectation is that if the contrast of the pre-compensated image is improved, the contrast of the final perceived image should also improve.

There exist several methods for enhancing the contrast of images. Such methods include amplitude scaling, histogram equalization, and adaptive histogram equalization (Pratt 2001). These methods rely on the statistics of the histogram to guide the enhancement process. The grey levels in the image may be regarded as a discrete random variable in the range [0, 1], assuming that the grey levels have been normalized so that 0 represents black and 1 represents white. Histogram processing seeks a transformation of the form

$$s = T(r) \qquad 0 \le r \le 1 \tag{11}$$

where r is the input grey level in the input image, and s is the resulting grey level after the transformation.

One of the most useful descriptors of a random variable, and thus of a digital image, is the probability density function (PDF) (Gonzales and Wood 2002). The PDF for a digital image can be approximated by

$$p_r(r_k) = \frac{n_k}{n} \quad k = 0, 1, 2, \ldots, L-1 \tag{12}$$

where n is the total number of pixels in the image, n_k is the number of pixels with grey level r_k, and L is the number of discrete grey levels. This is equivalent to the normalized histogram of the digital image (Gonzales and Wood 2002). Thus, the transformation to equalize the histogram, known as histogram equalization (HE) is given by

$$s_k = T(r_k) = \sum_{j=0}^{k} p_r(r_j) = \sum_{j=0}^{k} \frac{n_k}{n} \quad k = 0, 1, 2 \ldots, L-1. \tag{13}$$

This method was applied to the pre-compensated image shown in figure 5a (generated as described in the previous section), after the display scaling step. The results of the HE on figure 5a is shown in figure 6a. What the user would see while viewing the histogram-equalized pre-compensated (HEPC) image (figure 6a) through the aberration is shown in figure 6b. The contrast in the final viewed image of the HEPC image is greater than without histogram equalization. It was found however, that applying the HE prior to the intensity scaling step improves the contrast even more. Additionally, using a contrast limited adaptive histogram equalization (CLAHE) method, as described by Zuiderveld (1994), significantly improves the contrast. The CLAHE method was applied using the following parameters: the number of tiles to divide the image was chosen to be 2 x 2 or 4 tiles, the clip limit was 0.05, the distribution to match was a uniform distribution and the number of bins to equalize the histogram was 2 bins, essentially only black and white. The result of applying the CLAHE to figure 5a is shown in figure 7. The improvement in contrast is demonstrated through the histogram of the pre-compensated image viewed through the aberration with and without the application of contrast enhancement (figure 8).

It should be noted that figures 3, 5, 6, and 7 are software simulations using the methods outlined above. In order to demonstrate the method in a more realistic context, figures 9 a–d display pictures taken through a Sony MAVICA FD-900 digital camera simulating the visual system of a user interacting with the GUI. A fixed and known defocus was introduced in the field of view of the camera to simulate a visual aberration. Figure 9d confirms the ability of this method to preserve the acuity of the image. This enhancement of the effective visual acuity is likely to facilitate a user's interaction with the computer, as previous research has demonstrated that visual acuity is an important factor in the usability of GUIs by users with low vision (Jacko *et al*. 2000).

4. Evaluation

In order to assess the effectiveness of the pre-compensation with a known and fixed wavefront aberration, a −6 diopter spherical lens was interposed in the field of view of a digital camera (Sony Mavica MVC-FD95). This camera shows the image to the user in a 2.5″ LCD display with 800 x 225 pixel resolution.

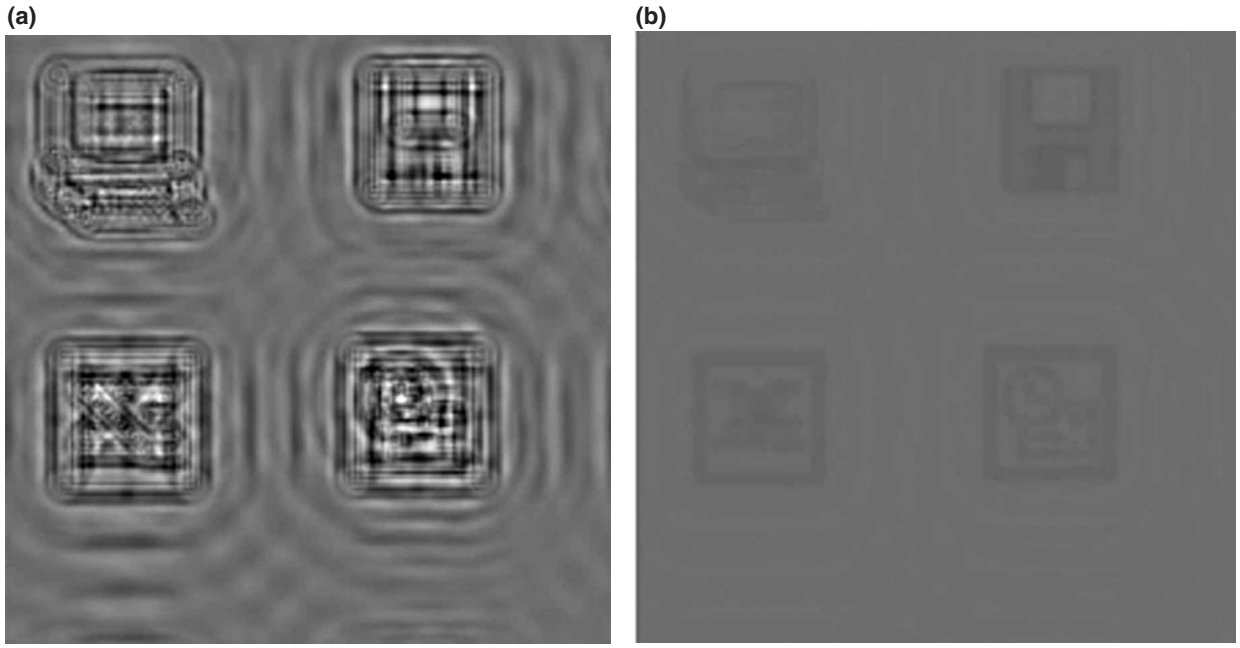

Figure 5(a). Result of pre-compensation (what is displayed to the user); (b) what the user with the aberration shown in figure 4 would perceive when viewing (a).

Since the ability to efficiently use an interface does not depend solely on the perception abilities of the user, but also involves higher-level cognitive processes to integrate and react to the perceptual input received, it was important to evaluate the potential gains of using pre-compensated images in a context that involved pattern recognition by human users. Accordingly, the evaluation of the system was performed by emulating a common visual acuity assess-

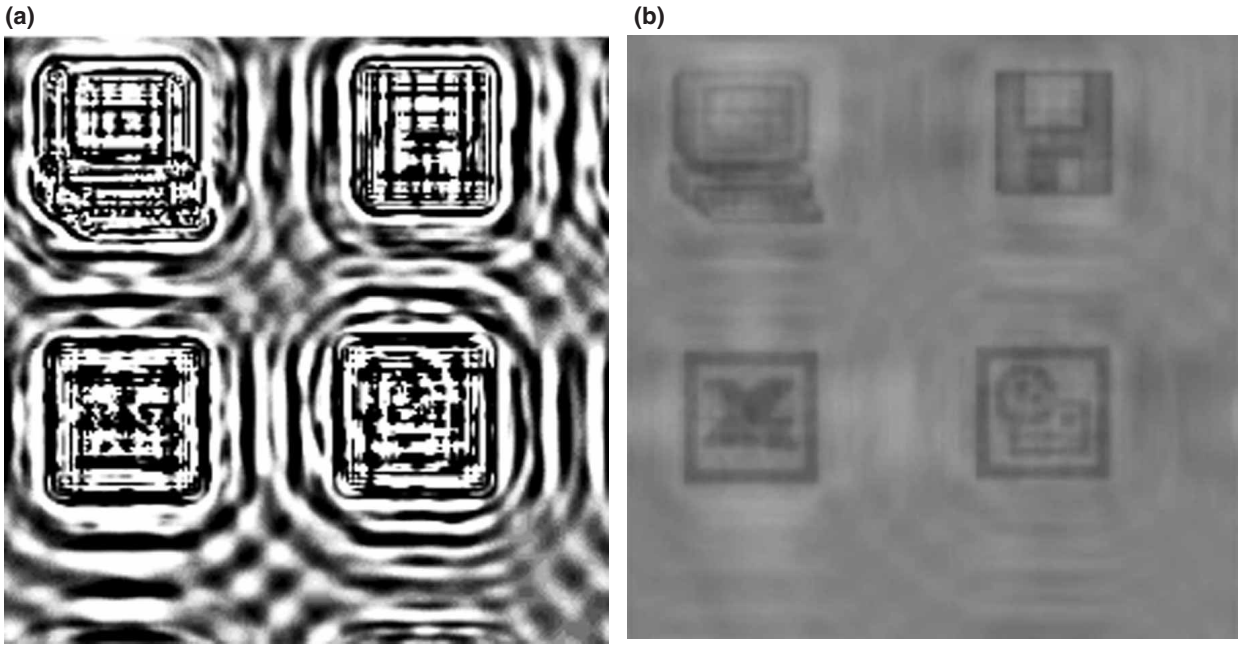

Figure 6(a). Result of pre-compensation (what is displayed to the user) with display scaling and histogram equalization; (b) what the user with the aberration shown in figure 4 would perceive when viewing (a).

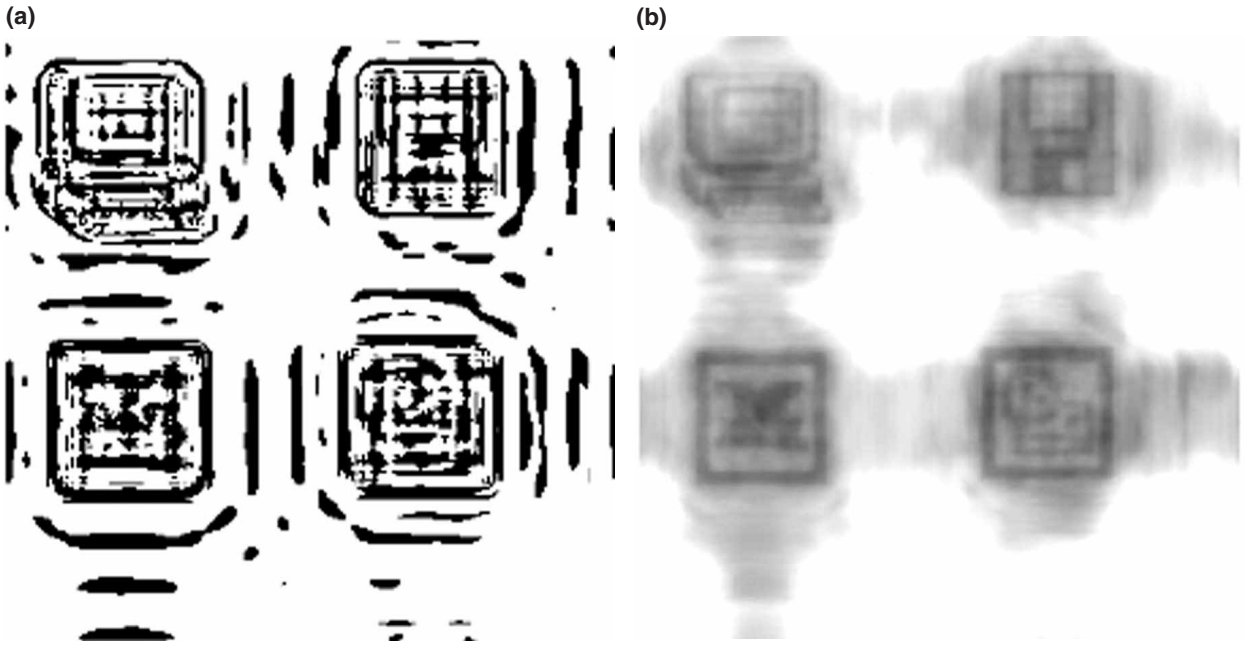

Figure 7(a). Result of pre-compensation (what is displayed to the user) with display scaling and CLAHE; (b) what the user with the aberration shown in figure 4 would perceive when viewing (a).

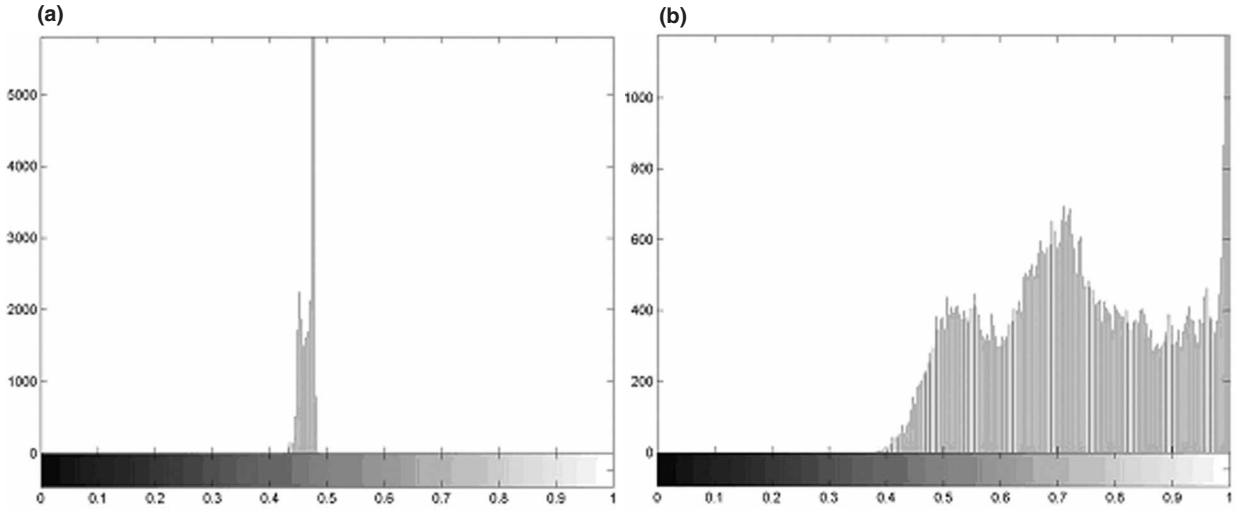

Figure 8(a). Histogram of figure 5b; (b) histogram of figure 7b.

ment, asking test subjects to recognize the letters on a Bailey-Lovie logMAR (logarithm of the minimum angle of resolution) eye test chart, with 'Sloan' letters (Bennet and Rabbetts 1989). This type of chart and its associated visual acuity measure (logMAR) were preferred over the Snellen visual acuity test chart because of several advantageous characteristics that would benefit this evaluation process (Bailey and Lovie 1976), namely:

The letter size progression is in uniform steps on a logarithmic scale so that the scaling factor is constant throughout the chart and will remain unaltered when non-standard viewing distances are used.

- Each row of the chart has the same number of letters (five).
- The letters present in all the lines are equally legible.
- Consistent spacing between letters (one letter width).
- Consistent spacing between rows (the space is equal to the height of letters in the smaller row).

In addition, Holladay (1997) has proposed that the logMAR units are the appropriate units to involve in statistical calculations of visual acuity. Figure 10 shows an example of a Bailey-Lovie logMAR chart.

4.1 *Evaluation levels*

The use of the digital camera with the fixed -6 diopter lens ensured that the wavefront aberration for all the experimental subjects would be the same. This allows for the same set of pre-compensated images to be used for all the subjects. On the other hand, this also introduced an inherent acuity limit. At the chosen test distance of 2 metres, the bars making up the letters of a given line in the chart have a specific width. When viewed through the limited resolution of the LCD display panel in the digital camera, the segments of the smallest letters (lines 13 and 14, with nominal logMAR values of -0.2 and -0.3 for the default viewing distance of 4 meters) will not be resolved in the display. This instrumental limitation made it necessary to also ask the subjects to read the letters in the chart without the blurring lens interposed in the field of view, defining the 'baseline acuity' for subjects with corrected vision in this instrumental setup.

Therefore, participating subjects viewed the simulated eye chart displayed on a computer monitor under three different conditions:

Standard: the (focused) digital camera was used to view the computer monitor without any interposed blurring lens. Normal images, emulating individual lines of the Bailey-Lovie chart were displayed.
Blurred: the -6 diopter blurring lens was placed in front of the camera. Normal images, emulating individual lines of the Bailey-Lovie chart were displayed.
Pre-compensated: the -6 diopter blurring lens was placed in front of the camera. In this case, the images shown in the computer monitor were pre-compensated versions of the original Bailey-Lovie rows, obtained using the PSF estimated for the -6 diopter spherical lens.

4.2 *Hypothesis*

The hypothesis explored through this experimentation was:

The display of pre-compensated digital images, as opposed to normal or 'direct' images, will result in a significantly better effective visual acuity.

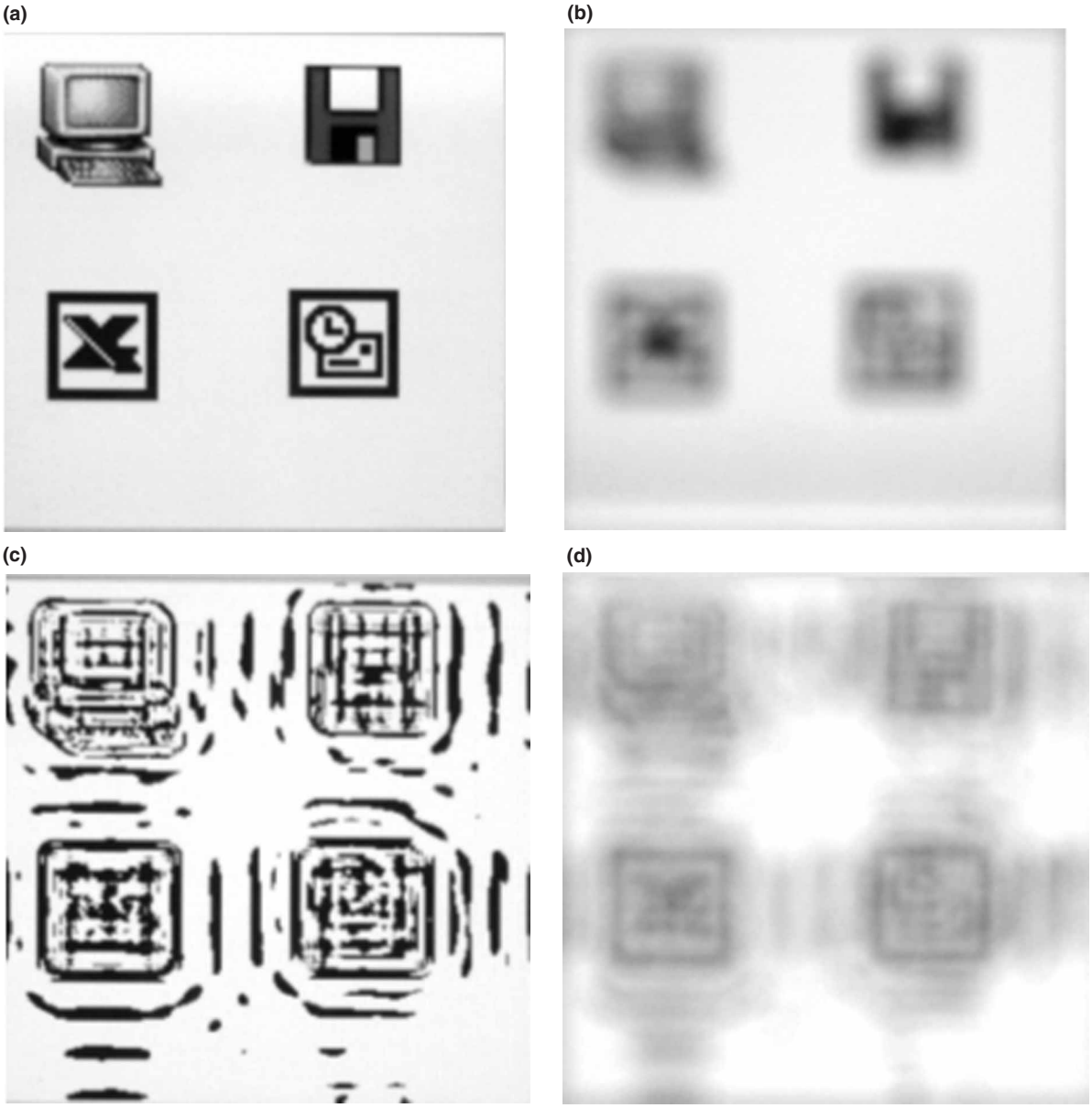

Figure 9(a). Intended image captured by the camera, without blur; (b) intended image captured by the camera, with blur; (c) pre-compensated image captured by the camera, without blur; (d) pre-compensated image captured by the camera, with blur.

4.3 *Subjects*

Fourteen college student volunteers (nine male and five female) participated in the evaluation of the system. Approval from the Institutional Review Board at Florida International University was obtained for this experiment involving human subjects. Each individual participant was briefed on the steps involved in the experiment and provided informed consent to the participation.

Since logMAR acuity is commonly evaluated on a monocular basis for clinical purposes, the evaluation performed for this research was also monocular. A total of 28 eyes were involved in the tests, and each was identified by a numerical 'Eye ID'. All of the participants were asked to use their spectacles or contact lenses and were considered to have fully corrected vision. Therefore, the pre-compensated images were developed on the assumption that the -6 diopter lens would introduce the totality of the wavefront aberration that needed to be

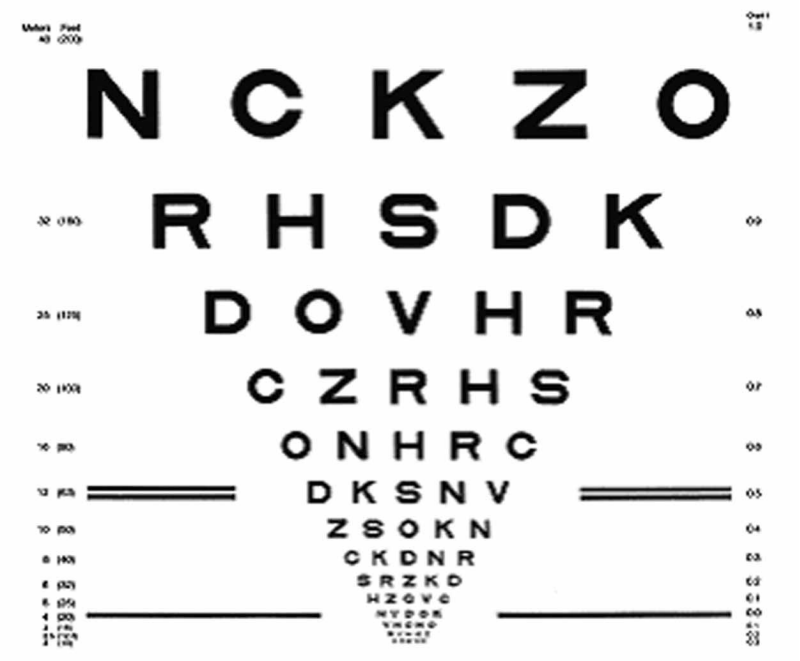

Figure 10. An example of a Bailey-Love logMAR eye test chart using 'sloan' letters.

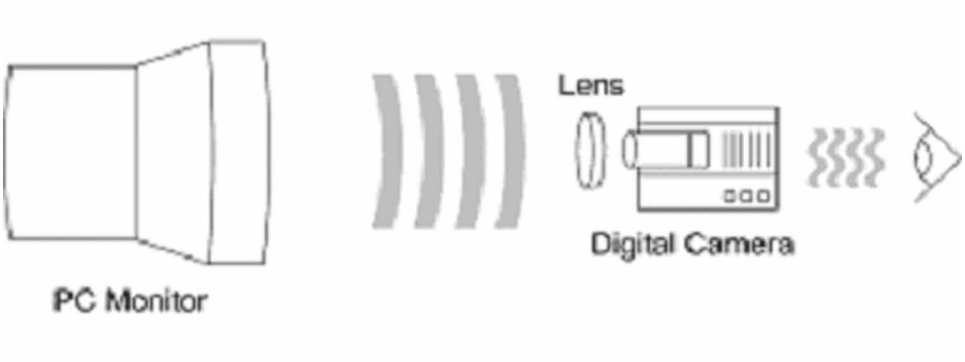

Figure 11. General instrumental setup for the evaluation process.

compensated. None of the subjects reported uncorrected visual limitations.

4.4 *Procedure*

Each subject was asked to view and read the simulated rows of the Bailey-Lovie chart from the computer monitor by looking at the LCD panel in the back of the digital camera. The participant would continue reading complete rows down the chart until errors were made, under each one of the three conditions identified above: standard, blurred and pre-compensated, first with one eye and then with the other. The order of this eye sequence was randomized. The sequence of the conditions implemented for each subject was also randomized. Figure 11 shows the instrumental configuration used (the lens was not used for the 'standard' experimental condition).

5. Results

5.1 *Measurements*

For each reading of the Bailey-Lovie chart the letters correctly read and those incorrectly read were recorded and the corresponding logMAR score (corrected for the chosen

testing distance of 2 metres) was calculated. To determine the true logMAR value, X, in a case in which the subject correctly read the complete row corresponding to a logMAR value cLV, and only $n < 5$ letters from the next line, the following formula can be used (Holladay 1997):

$$X = cLV - 0.1(n/5). \tag{14}$$

Once the logMAR value X is determined, the 'decimal acuity', V, can be found as (Holladay 1997):

$$V = 10^{-X} \tag{15}$$

and the, so-called 'visual efficiency', E, defined by the American Medical Association, can be found through the following equations (Bennet and Rabbetts 1989)

$$\log E = -0.0777A + 2.0777 \tag{16}$$

$$A = \frac{2.0777 - \log E}{0.0777} \tag{17}$$

where

$$A = 1/V. \tag{18}$$

Table 1 displays the mean and standard deviation of the logMAR values recorded from the 28 eyes studied, under each of the three experimental conditions. This table also includes the average visual efficiency value, and associated standard deviation, for each condition.

From the table it should be noted that although the pre-compensation did not fully return the performance of the subjects to the levels achieved in the unimpaired, 'standard' condition (mean logMAR = 0.33, $E = 81.39\%$), it indeed improved with respect to the severely restricted acuity observed for the impaired, uncompensated condition (blurred), which recorded a mean logMAR value of 1.37 and a mean visual efficiency of only $E = 1.92\%$.

With the display of pre-compensated images viewed through the blurring lens, the mean logMAR acuity and the mean visual efficiency reached values of 0.67 and 51.69%, respectively. The similarity of the behaviour across the 28 eyes studied, with respect to the three experimental conditions tested is shown in figure 12, which displays the

Table 1. Summary of the experimental results.

Experimental condition	LogMAR acuity		Visual efficiency	
	Mean	Std.dev.	Mean	Std.dev.
Standard	0.33	0.05	81.39%	3.38%
Blurred	1.37	0.05	1.92%	1.36%
Pre-compensated	0.67	0.04	51.69%	4.22%

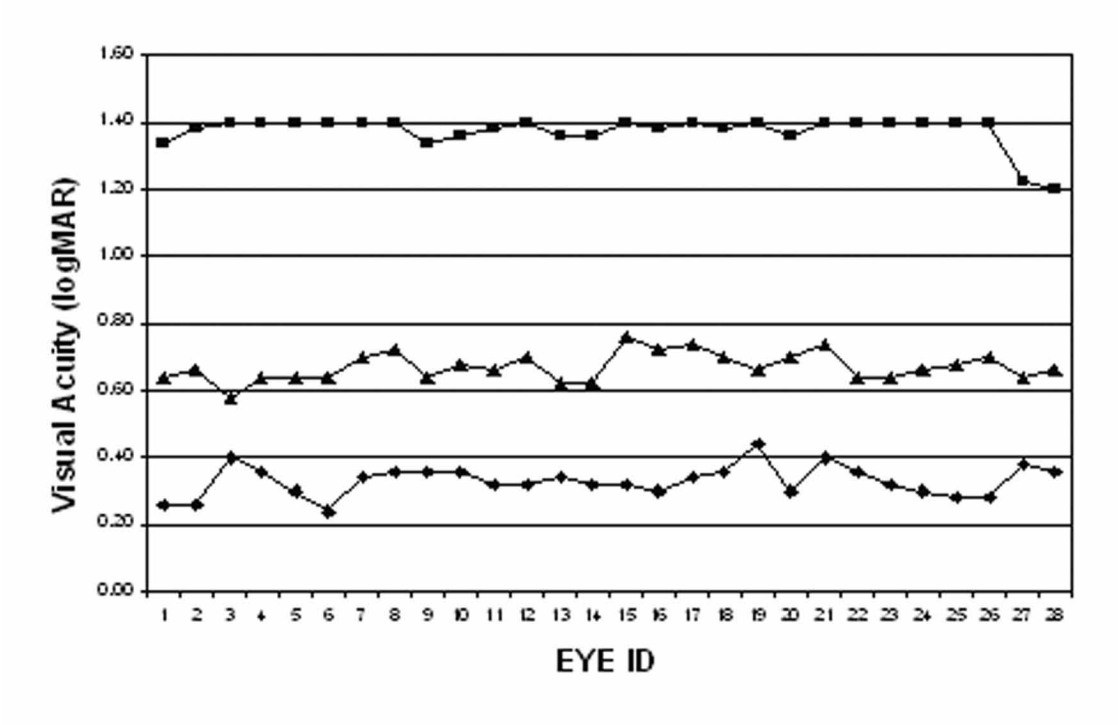

Figure 12. LogMAR acuity measurements under the three conditions tested: 'standard' (diamonds), 'blurred' (squares), and 'pre-compensated' (triangles).

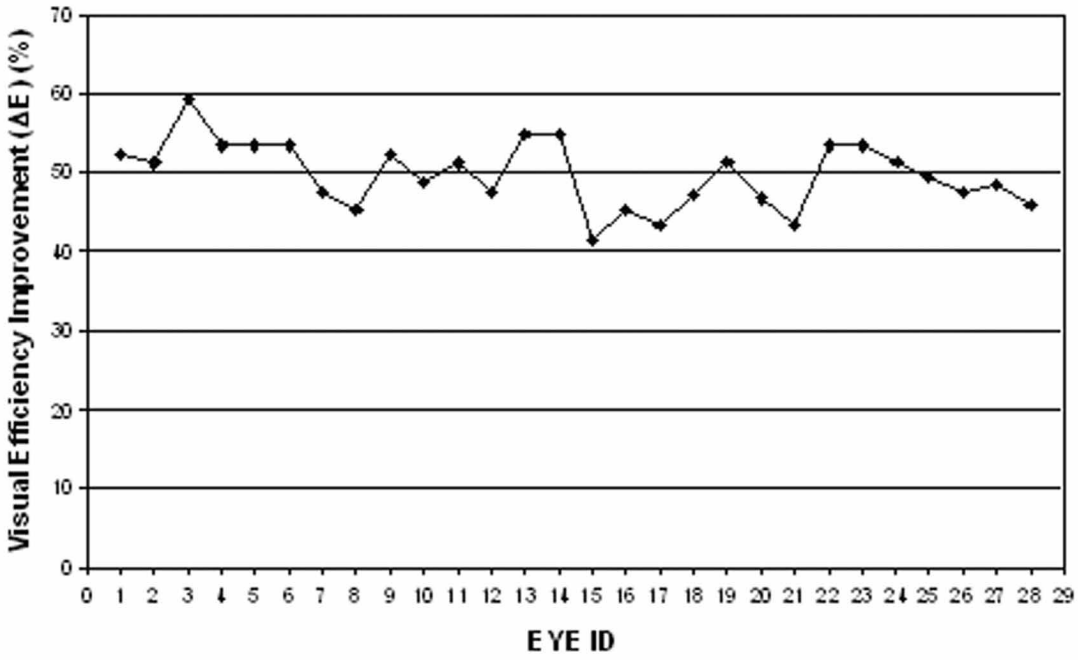

Figure 13. Visual efficiency enhancement, $\Delta E = E_{precomp} - E_{blurred}$, achieved by displaying pre-compensated images.

logMAR acuity values for all eyes under the three conditions.

In order to address the main question behind the experiment, the difference in visual efficiency for the two impaired viewing conditions established by the display of pre-compensated images or original (direct) images, i.e., $\Delta E = E_{\text{precomp}} - E_{\text{blurred}}$, was calculated for each one of the 28 eyes. Figure 13 displays these values.

5.2 *Data analysis*

A dependent t-test was performed using the Statistical Package for the Social Sciences (SPSS), V.9. The results confirmed that there was a significant difference ($t(27) = 64.89$, $p < 0.01$) in the logMAR acuity recorded when the direct images were displayed ('blurred' condition) and when the pre-compensated images were displayed ('pre-compensated' condition). The display of pre-compensated images considerably reduced the mean logMAR acuity from 1.37 to 0.67, and reduced the standard deviation of the logMAR measurements (from 0.05 to 0.04).

6. Conclusion

The simulations and imaging tests performed with a digital camera have illustrated the potential of the image pre-compensation approach proposed to revert the degradation on the perception of visual interface elements. Additional enhancement of the contrast of the pre-compensated image using CLAHE resulted in a higher contrast when the pre-compensated image is viewed through the aberration. Furthermore, the evaluation conducted with human subjects resulted in improved visual acuity scores recorded when the pre-compensated images were used. The statistical analysis performed on the experimental data supports the hypothesis that displaying the pre-compensated images provides a significant enhancement of the effective visual acuity of the user.

The next stage of our work will use the methods developed to generate the pre-compensation for participants with targeted visual impairments, preferably of high-order. This will allow verification of the general applicability of the algorithms.

We envisage that this pre-compensation approach will be applicable to users with severe refractive errors whose individual wavefront aberration functions can be obtained using wavefront analysers, as these instruments are becoming a common tool used by many ophthalmologists and optometrists.

Acknowledgements

This work was sponsored by National Science Foundation (NSF) grants IIS-0308155, CNS-0426125 and HRD-

0317692. Mr Miguel Alonso Jr is the recipient of an NSF Graduate Research Fellowship.

References

Bailey, I.L. and Lovie, J.E., 1976, New design principles for visual acuity charts. *American Journal of Optometry*, **57,** 378–387.

Bennet, A.G. and Rabbetts, R.B., 1989, *Clinical Visual Optics* (London: Butterworths).

Gonsalves, R.A. and Nisenson, P., 1991, Host image processing: an overview of algorithms for image restoration. *SPIE Applications of Digital Image Processing*, **1567,** 294–307.

Gonzales, R.C. and Wood, R.E., 2002, *Digital Image Processing* (New Jersey: Prentice Hall).

Goodman, J.W., 1968, *Introduction to Fourier Optics* (New York: McGraw-Hill).

Guyton, A.C. and Hall, J.E., 1996, *Textbook of Medical Physiology* (Philadelphia: Saunders).

Higuchi, K., Nakano, T. and Yamamoto, S., 2000, Simulating human vision based on adaptation and age-related visual changes. *R and D Review of Toyota CRDL*, **35**.

Hjortdal, J., 2003, Book review: wavefront and emerging refractive technology. *ACTA Ophthalmologica Scandanavia*, **81,** 681.

Holladay, J.T., 1997, Proper method for calculating average visual acuity. *Journal of Refractive Surgery*, **13,** 388–391.

Jacko, J.A., Barreto, A.B., Marmet, G.J., Chu, J.Y., Bautsch, H.S., Scott, I.U. and Rosa, R.H., 2000, Low vision: the role of visual acuity in the efficiency of cursor movement. *Fourth International ACM Conference on Assistive Technologies (ASSETS '00)*, 13–15 November 2000 (Arlington, VA: ACM), pp. 1–7.

Kline, R.L. and Glinert, E.P., 1995, Improving GUI accessibility for people with low vision. *CHI'95 Conference on Human Factors in Computing Systems*, (New York: ACM), pp. 114–121.

Liang, J., Grimm, B., Goelz, S. and Bille, J.F., 1994, Objective measurement of wave aberrations of the human eye with the use of a Hartmann-Shack wave-front sensor. *Journal of the Optical Society of America*, **11,** 1949–1957.

Liang, J., Williams, D.R. and Miller, D.T., 1997, Supernormal vision and high-resolution retinal imaging through adaptive optics. *Journal of the Optical Society of America*, **14,** 2884–2892.

Parker, J.N. and Parker, P.M., 2002, *The Official Patient's Sourcebook on Keratoconus: A Revised and Updated Directory for the Internet Age* (San Diego: Icon Health Publications).

Pratt, W.K., 2001, *Digital Image Processing* (New York: John Wiley & Sons).

Salmon, T.O., 1999, *Corneal Contribution to the Wavefront Aberration of the Eye* (Bloomington: Indiana University).

Thibos, L.N., 2000, Formation and sampling of the retinal image. In *Seeing: Handbook of Perception and Cognition*, K. K. D. Valois (Ed.) pp. 1–54 (San Diego: Academic Press).

Thibos, L.N., Qi, X. and Miller, D.T., 1999, Vision through a liquid crystal spatial light modulator. *2nd International Workshop on Adaptive Optics for Industry and Medicine*, (Singapore: World Scientific Press), pp. 57–62.

Williams, C.S. and Becklund, O.A., 1989, *Introduction to the Optical Transfer Function* (New York: John Wiley & Sons).

Wilson, R.G., 1995, *Fourier Series and Optical Transform Techniques in Contemporary Optics: An Introduction* (New York: John Wiley & Sons).

Young, M., 2003, AAO preview: a close look at wavefront. *EyeWorld*, September, **30**.

Zuiderveld, K., 1994, Contrast limited adaptive histogram equalization. In *Graphic Gems,* P. Heckbert (Ed.), pp. 474–485 (London: Academic Press).